# A General Truncated Regularization Framework for Contrast-Preserving Variational Signal and Image Restoration: Motivation and Implementation

WU ChunLin
(Joint work with LIU ZhiFang, WEN Shuang)

School of Mathematical Sciences, Nankai University, Tianjin 300071, China

NJUPT, Nanjing, April, 14, 2018

# Outline

# Section 1. Variational signal and image restoration

# Variational signal and image restoration - signal degradation

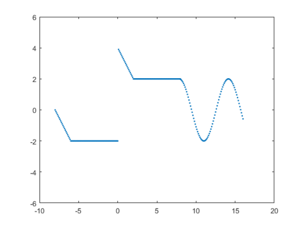


true image

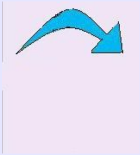

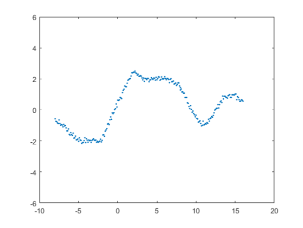


noisy observation

# Variational signal and image restoration - signal restoration

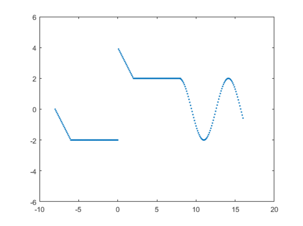

true image

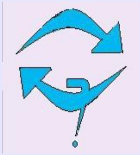

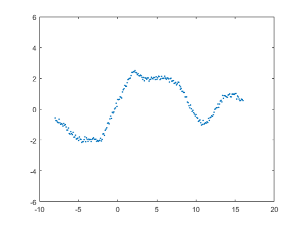

noisy observation

# Variational signal and image restoration - image degradation

true image

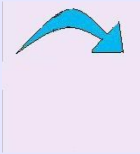

blurred and noisy observation

# Variational signal and image restoration - image restoration

true image

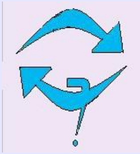

blurred and noisy observation

# Variational signal and image restoration - 1D signal

- 1D signal $f \in \mathbb{R}^K$ is a degradation of $\underline{u} \in \mathbb{R}^N$:

$$\underline{u} \to A\underline{u} \xrightarrow{n} f,$$

- $A$ is a linear operator such as a blur convolution.
- $n = \{n_i : 1 \leq i \leq K\}$ is random noise.
- $n_i \sim \mathcal{N}(0, \sigma^2), 1 \leq i \leq K$ are i.i.d. random variables, such as additive Gaussian noise and multiplicative noise.

# Variational signal and image restoration - general model for signal restoration

$$\min_{u\in\mathbb{R}^N}\left\{\begin{aligned} E(u) &= \sum_{1\leq i\leq N}\varphi((\nabla_x u)_i) + \frac{\alpha}{2}\|Au-f\|^2_{\mathbb{R}^K} \\ &= \sum_{1\leq i\leq N}\rho(|(\nabla_x u)_i|) + \frac{\alpha}{2}\|Au-f\|^2_{\mathbb{R}^K}\end{aligned}\right\}, \tag{1}$$

- $\rho(\cdot)$ is a potential function.
- $\nabla_x$ is the forward difference operator with a specific boundary condition, e.g., the periodic or Neumann boundary condition.

# Variational signal and image restoration - 2D image

- 2D image $\mathbf{f} \in \mathbb{R}^{K \times K}$ is a degradation of $\underline{\mathbf{u}} \in \mathbb{R}^{N \times N}$:

$$\underline{\mathbf{u}} \rightarrow \mathbf{A}\underline{\mathbf{u}} \xrightarrow{\mathbf{n}} \mathbf{f},$$

- $\mathbf{A}$ is a linear operator such as a blur convolution.
- $\mathbf{n} = \{\mathbf{n}_{i,j}, 1 \leq i,j \leq K\}$ is random noise.
- $\{\mathbf{n}_{i,j} \sim \mathcal{N}(0, \sigma^2), 1 \leq i,j \leq K\}$ are i.i.d. random variables, such as additive Gaussian noise and multiplicative noise.

# Variational signal and image restoration - general model for image restoration

$$\min_{\mathbf{u}\in\mathbb{R}^{N\times N}} \left\{ \begin{aligned} E_{\text{ani}}(\mathbf{u}) &= \sum_{1\le i,j\le N} (\varphi((\nabla_x \mathbf{u})_{i,j}) + \varphi((\nabla_y \mathbf{u})_{i,j})) + \frac{\alpha}{2}\|\mathbf{A}\mathbf{u}-\mathbf{f}\|^2_{\mathbb{R}^{K\times K}} \\ &= \sum_{1\le i,j\le N} (\rho(|(\nabla_x \mathbf{u})_{i,j}|) + \rho(|(\nabla_y \mathbf{u})_{i,j}|)) + \frac{\alpha}{2}\|\mathbf{A}\mathbf{u}-\mathbf{f}\|^2_{\mathbb{R}^{K\times K}} \end{aligned} \right\}, \tag{2}$$

$$\min_{\mathbf{u}\in\mathbb{R}^{N\times N}} \left\{ \begin{aligned} E_{\text{iso}}(\mathbf{u}) &= \sum_{1\le i,j\le N} \psi((\nabla_x \mathbf{u})_{i,j}, (\nabla_y \mathbf{u})_{i,j}) + \frac{\alpha}{2}\|\mathbf{A}\mathbf{u}-\mathbf{f}\|^2_{\mathbb{R}^{K\times K}} \\ &= \sum_{1\le i,j\le N} \rho(\sqrt{(\nabla_x \mathbf{u})^2_{i,j} + (\nabla_y \mathbf{u})^2_{i,j}}) + \frac{\alpha}{2}\|\mathbf{A}\mathbf{u}-\mathbf{f}\|^2_{\mathbb{R}^{K\times K}} \end{aligned} \right\}, \tag{3}$$

- $\nabla_x$ and $\nabla_y$ are the forward difference operators with a specific boundary condition.

# Section 2. Assumptions on potential functions $\rho(\cdot)$

# Assumptions on potential functions $\rho(\cdot)$

(AS1) $\rho(0) = 0, \rho(s) < +\infty, \forall s < +\infty$ with 0 as its strict minimizer;

(AS2) $\rho(s)$ is increasing over $[0, \infty)$;

(AS3) $\rho(s)$ is $C^2$ on $(0, +\infty)$;

(AS4) $\rho''(s) < 0$ strictly increases on $(0, +\infty)$ or $\rho''(s) \equiv 0$ on $(0, +\infty)$.

# Assumptions on potential functions $\rho(\cdot)$ - some potential functions

when $0 < p < 1, \theta > 0, a > 2$

$\rho_1(s) = s$

$\rho_2(s) = s^p$

$\rho_3(s) = \ln(\theta s + 1)$

$\rho_4(s) = \frac{\theta s}{1+\theta s}$

$\rho_5(0) = 0, \rho_5(s) = 1$ if $s > 0$

$\rho_6(s) = \ln(\theta s^p + 1)$

$\rho_7(s) = \frac{\theta s^p}{1+\theta s^p}$

$$\rho_8(s) = \begin{cases} \theta s, & s \leq \theta \\ \frac{-s^2-\theta^2+2a\theta s}{2(a-1)}, & \theta < s < a\theta \\ \frac{(a+1)\theta^2}{2}, & s > a\theta \end{cases}$$

when $p > 1, \theta > 0.$

$\rho_9(s) = min\{\theta s^2, 1\}$

$\rho_2(s) = s^p$

$\rho_7(s) = \frac{\theta s^p}{1+\theta s^p}$

# Section 3. Nonconvex regularization: Motivation

# Nonconvex regularization: Motivation

- Key features of signals and images:
    - Edges
    - Contrasts
- Convex regularizer is impossible to perfectly recover a nonconstant signal.

# Nonconvex regularization: Motivation - 1D signal

## Proposition

*Assume* $\rho(\cdot)$ *to be convex and satisfy (AS1)(AS2). If a signal* $\tilde{u} \in \mathbb{R}^N$ *can be recovered by the minimization problem* (1) *with* $f = A\tilde{u}$, *then* $\tilde{u} \in \mathbb{R}^N$ *is a constant signal, i.e.,* $\tilde{u} = c(1, 1, \cdots, 1) \in \mathbb{R}^N$ *for some* $c \in \mathbb{R}$.

# Section 4. Truncated regularization framework

# Truncated regularization framework

A new regularizer function

$$\overline{T}(\cdot) = \rho_\tau(\cdot) = \rho(\min(\cdot, \tau)), \tag{4}$$

- $\tau > 0$ is a positive real parameter.
- Flat on $(\tau, +\infty)$.
- If $\rho(\cdot)$ satisfies the basic assumptions (AS1)(AS2), $\overline{T}(\cdot) = \rho_\tau(\cdot)$ also satisfies the basic assumptions (AS1)(AS2).
- $\overline{T}(\cdot)$ is always nonconvex.

# Truncated regularization framework - subadditivity of min function

## Lemma

*Given* $a, b \geq 0, \tau > 0$, *then*

$$\min(a+b, \tau) \leq \min(a, \tau) + \min(b, \tau). \tag{5}$$

## Proposition

*Given* $\tau > 0$, *if* $\rho(\cdot)$ *satisfies the subadditivity property over* $[0, +\infty)$ *and the assumptions (AS1)(AS2), then its truncated version* $\overline{T}(\cdot) = \rho(\min(\cdot, \tau))$ *also has the subadditivity property over* $[0, +\infty)$.

# Section 5. Theoretical justification in 1D

# Theoretical justification in 1D - truncated regularization in 1D signal

- $\emptyset \neq \Omega \subsetneq J = \{1, \cdots, N\}$.
- $\mathbf{1}_\Omega$ be its indicator function and $\zeta > 0$ be a real number.
- $J_0 = \{i : (\nabla_x \mathbf{1}_\Omega)_i = 0\}$.
- $J_1 = \{i : (\nabla_x \mathbf{1}_\Omega)_i \neq 0\} = J \setminus J_0$.

Consider now the minimization problem (1) using truncated regularization where $f = A(\zeta \mathbf{1}_\Omega) \in \mathbb{R}^K$. Denote

$$E^\zeta(u) = \sum_{1 \leq i \leq N} \overline{T}(|(\nabla_x u)_i|) + \frac{\alpha}{2} \|A(u - \zeta \mathbf{1}_\Omega)\|^2_{\mathbb{R}^K}. \tag{6}$$

# Theoretical justification in 1D - perfect recovery of 1D signal

The following theorem shows the perfect recovery (i.e., contrast preservation) of the signal $\zeta \mathbf{1}_\Omega$ by (1) with a truncated regularization.

## Theorem

*If $\zeta > \tau + \sqrt{\frac{4\overline{T}(\tau)}{\alpha \mu_{\min}} \# J_1}$, then the global minimizer is $\zeta \mathbf{1}_\Omega$. Here $\mu_{\min} > 0$ is the minimal eigenvalue of $A^T A$.*

# Theoretical justification in 1D - perfect recovery of 1D signal

## Theorem

*Assume* $A^TA = diag\{d_1, d_2, \cdots, d_N\}, d_i > 0, i = 1, 2, \cdots, N$ *and the regularizer function* $\overline{T}(\cdot)$ *in* (6) *to satisfy the subadditivity (Note here we do not require the finiteness of* $\tau$*). Let* $v$ *be the global minimizer of* (6), *then*

(1) *The extremum principle holds, i.e.,* $0 \leq v_i \leq \zeta$ *for all* $i \in J$*;*

(2) *No new (and thus false) discontinuity appears in* $v$*, i.e.,* $J_1^* = \{i \in J : (\nabla_x v)_i \neq 0\} \subseteq J_1$*;*

(3) $v$ *preserves the monotonicity (not necessarily strict) from the input signal* $\zeta\mathbf{1}_\Omega$.

# Section 6. Numerical demonstration in 2D

# Numerical demonstration in 2D
# - truncated regularization in 2D image

- *Anisotropic 2D truncated regularization model*:

$$\min_{\mathbf{u}\in V}\left\{E_{\text{ani}}^{\overline{T}}(\mathbf{u})=\sum_{1\leq i,j\leq N}\overline{T}(|(\nabla_x\mathbf{u})_{ij}|)+\overline{T}(|(\nabla_y\mathbf{u})_{ij}|)+\frac{\alpha}{2}\|\mathbf{Au}-\mathbf{f}\|_V^2\right\},\tag{7}$$

- *Isotropic 2D truncated regularization model*:

$$\min_{\mathbf{u}\in V}\left\{E_{\text{iso}}^{\overline{T}}(\mathbf{u})=\sum_{1\leq i,j\leq N}\overline{T}\left(\sqrt{(\nabla_x\mathbf{u})_{ij}^2+(\nabla_y\mathbf{u})_{ij}^2}\right)+\frac{\alpha}{2}\|\mathbf{Au}-\mathbf{f}\|_V^2\right\},\tag{8}$$

which are truncated versions of (2) and (3), respectively.

# Numerical demonstration in 2D - ADMM solver

Constrained optimization problem:

$$\min_{(\mathbf{u},\mathbf{q})\in V\times Q} \left\{ \tilde{E}_{\text{iso}}^{\overline{T}}(\mathbf{u},\mathbf{q}) = \sum_{1\le i,j\le N} \overline{T}(|\mathbf{q}_{ij}|) + \frac{\alpha}{2}\|\mathbf{A}\mathbf{u}-\mathbf{f}\|_V^2 \right\}, \tag{9}$$
$$\text{s.t.} \qquad \mathbf{q} = (\nabla_x \mathbf{u}, \nabla_y \mathbf{u}).$$

The augmented Lagrangian functional for the problem (9):

$$\begin{aligned}\mathcal{L}(\mathbf{u},\mathbf{q};\boldsymbol{\lambda}) &= \sum_{1\le i,j\le N} \overline{T}(|\mathbf{q}_{ij}|) + \frac{\alpha}{2}\|\mathbf{A}\mathbf{u}-\mathbf{f}\|_V^2 + (\boldsymbol{\lambda}, \mathbf{q}-\nabla\mathbf{u})_Q + \frac{\beta}{2}\|\mathbf{q}-\nabla\mathbf{u}\|_Q^2 \\ &= R(\mathbf{q}) + \frac{\alpha}{2}\|\mathbf{A}\mathbf{u}-\mathbf{f}\|_V^2 + (\boldsymbol{\lambda}, \mathbf{q}-\nabla\mathbf{u})_Q + \frac{\beta}{2}\|\mathbf{q}-\nabla\mathbf{u}\|_Q^2,\end{aligned}$$

- $\nabla\mathbf{u} = (\nabla_x\mathbf{u}, \nabla_y\mathbf{u})$;
- $\boldsymbol{\lambda} \in Q$ is the Lagrangian multiplier, $\beta > 0$ is a constant;
- $R(\mathbf{q})$ is introduced to simply the notation of the regularization term.

# Numerical demonstration in 2D - algorithm for (8)

Initialization: $\mathbf{u}^0, \mathbf{q}^0, \boldsymbol{\lambda}^0$;
**while** stopping criteria is not satisfied **do**
    Compute $\mathbf{q}^{k+1}$, $\mathbf{u}^{k+1}$, and update $\boldsymbol{\lambda}^{k+1}$ as follows:

$$\mathbf{q}^{k+1} \in \underset{\mathbf{q}\in Q}{\operatorname{argmin}}\, \mathcal{L}(\mathbf{u}^k, \mathbf{q}; \boldsymbol{\lambda}^k), \tag{10}$$

$$\mathbf{u}^{k+1} = \underset{\mathbf{u}\in V}{\operatorname{argmin}}\, \mathcal{L}(\mathbf{u}, \mathbf{q}^{k+1}; \boldsymbol{\lambda}^k), \tag{11}$$

$$\boldsymbol{\lambda}^{k+1} = \boldsymbol{\lambda}^k + \beta(\mathbf{q}^{k+1} - \nabla\mathbf{u}^{k+1}), \tag{12}$$

**end while**

# Numerical demonstration in 2D - u$-$sub problem (11)

The $\mathbf{u}-$sub problem (11) is a quadratic optimization problem, whose optimality condition gives a linear system

$$\alpha \mathbf{A}^\mathsf{T}(\mathbf{A}\mathbf{u} - \mathbf{f}) - \nabla^\mathsf{T}\boldsymbol{\lambda}^k - \beta\nabla^\mathsf{T}\mathbf{q}^{k+1} - \beta\Delta\mathbf{u} = 0,$$

which can be solved by Fourier transform with an FFT implementation.

# Numerical demonstration in 2D - q−sub problem (10)

The problem (10) reads

$$\min_{\mathbf{q}\in Q}\left\{\sum_{1\le i,j\le N}\overline{T}(|\mathbf{q}_{ij}|)+(\boldsymbol{\lambda}^k,\mathbf{q}-\nabla\mathbf{u}^k)_Q+\frac{\beta}{2}\|\mathbf{q}-\nabla\mathbf{u}^k\|_Q^2\right\},$$

which, by the monotonicity of $\rho$ over $[0,+\infty)$, is

$$\min_{\mathbf{q}\in Q}\left\{\sum_{1\le i,j\le N}\min\big(\rho(|\mathbf{q}_{ij}|),\rho(\tau)\big)+\frac{\beta}{2}|\mathbf{q}_{i,j}-\mathbf{w}_{i,j}|^2\right\},$$

where $\mathbf{w}=\nabla\mathbf{u}^k-\boldsymbol{\lambda}^k/\beta\in Q$. This problem is separable.

$$\min_{z\in\mathbb{R}^2}\left\{g(z;w)=\min\big(\rho(|z|),\rho(\tau)\big)+\frac{\beta}{2}|z-w|^2\right\},$$

where $|z|=\sqrt{(z^{(1)})^2+(z^{(2)})^2}$; and $w\in\mathbb{R}^2,\tau>0,\beta>0$ are given.

# Numerical demonstration in 2D - q$-$sub problem (10) Cont.

Suppose $z^* = \operatorname*{argmin}_{z\in\mathbb{R}^2} g(z;w)$.

- If $w = (0,0)$, it is clear that $z^* = (0,0)$.
- For $w$ with $|w| \neq 0$, $z^*$ has the same direction as $w$: $z^* = \frac{|z^*|}{|w|}w$. Thus to obtain $z^*$, it is sufficient to calculate $|z^*|$ as the minimizer of the following univariate problem:

$$\min_{s\geq 0}\left\{\chi(s;\tau,\beta,t) = \min\big(\rho(s),\rho(\tau)\big) + \frac{\beta}{2}(s-t)^2\right\}, \qquad (13)$$

where $t = |w|$.

# Numerical demonstration in 2D - q−sub problem (10) Cont.

For the convenience of description, we introduce the following two functions

$$\chi_1(s) = \rho(s) + \frac{\beta}{2}(s - t)^2, \tag{14}$$

$$\chi_2(s) = \rho(\tau) + \frac{\beta}{2}(s - t)^2. \tag{15}$$

# Numerical demonstration in 2D - q−sub problem (10) Cont.

## Proposition

*The minimization problem* (13) *can be solved by*

$$s^* = \begin{cases} s_1^*, & \chi_1(s_1^*) < \chi_2(s_2^*), \\ \{s_1^*, s_2^*\}, & \chi_1(s_1^*) = \chi_2(s_2^*), \\ s_2^*, & \chi_1(s_1^*) > \chi_2(s_2^*), \end{cases} \tag{16}$$

*where*

$$s_1^* = \operatorname*{argmin}_{0 \le s \le \tau} \chi_1(s); s_2^* = \operatorname*{argmin}_{s \ge \tau} \chi_2(s) = \max(t, \tau).$$

# Numerical demonstration in 2D - q−sub problem (10) Cont.

## Proposition

*[second order lower bound] If $\rho(\cdot)$ satisfies (AS1)(AS2)(AS3)(AS4) and $s^*_{loc}$ is a local minimizer of $\min_{s\geq 0} \chi_1(s)$, then either $s^*_{loc} = 0$ or $s^*_{loc} \geq s_L$.*

## Proposition

*Under the assumptions of Proposition above, we have:*

(1) *If $s_L > 0, \chi_1'(s_L) \geq 0$ ($s_L = 0, \chi_1'(0+) \geq 0$), then $s_1^* = 0$ is the unique global minimizer of $\min_{0\leq s\leq \tau} \chi_1(s)$.*

(2) *If $s_L > 0, \chi_1'(s_L) < 0$ ($s_L = 0, \chi_1'(0+) < 0$), then the equation $\chi_1'(s) = 0$ has a unique root $\bar{s}$ on $[s_L, t]$. Set $\mathcal{X} = \{0, \min(\bar{s}, \tau)\}$. The global minimizer of $\min_{0\leq s\leq \tau} \chi_1(s)$ is given by $s_1^* = \arg\min_{s\in\mathcal{X}} \chi_1(s)$.*

# Numerical demonstration in 2D - algorithm for solving (13)

**Require:** $t$, $\tau$, the second order bound $s_L$ and functions $\chi_1(s)$, $\chi_1'(s+)$, $\chi_2(s)$;

**Ensure:** $s^*$;

```
// Find the global minimizer of s_1^* = arg min_{0≤s≤τ} χ_1(s).
if χ_1'(s_L+) < 0 then
    Find the root s̄ of equation χ_1'(s) = 0 in [s_L, t];
    Set the feasible set 𝒳 = {0, min(s̄, τ)};
    Choose s_1^* ∈ 𝒳 with s_1^* := arg min_{s∈𝒳} χ_1(s);
else
    Set s_1^* = 0;
end if
// Find the global minimizer of s_2^* = arg min_{t≤τ} χ_2(s).
Set s_2^* = max{τ, t};
// Find the global minimizer s^*.
Choose s^* with
```

$$s^* = \begin{cases} s_1^*, & \chi_1(s_1^*) < \chi_2(s_2^*), \\ \{s_1^*, s_2^*\}, & \chi_1(s_1^*) = \chi_2(s_2^*), \\ s_2^*, & \text{otherwise}. \end{cases}$$

# Numerical demonstration in 2D - convergence analysis

(AS5) $A^{\mathsf{T}}A$ ($\mathbf{A}^{\mathsf{T}}\mathbf{A}$) is invertible.

## Theorem

*Assume that (AS1)(AS2)(AS3)(AS4)(AS5) hold and* $\boldsymbol{\lambda}^{k+1} - \boldsymbol{\lambda}^{k} \to 0$ *as* $k \to \infty$ *in the ADMM. Then any cluster point of the sequence* $\{(\mathbf{u}^k, \mathbf{q}^k, \boldsymbol{\lambda}^k)\}$*, if exists, is a KKT point of the constrained optimization problem.*

# Numerical demonstration in 2D - experimental results

[Satellite. Size: 135 $\times$ 135]

[TV. PSNR: 23.30dB ]

[SCAD. PSNR: 24.11dB ]

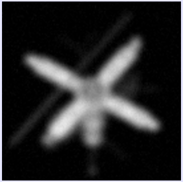

[Blurry & Noisy. PSNR: 19.99dB]

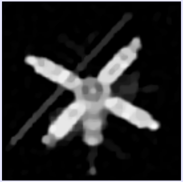

[TR-TV. PSNR: 23.95dB ]

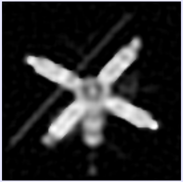

[TR-$\ell_2$. PSNR: 23.01dB ]

# Numerical demonstration in 2D - experimental results

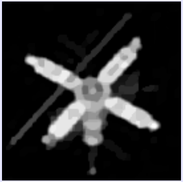

[$\ell_p$. PSNR: 23.93dB]

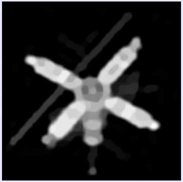

[LN. PSNR: 23.77dB]

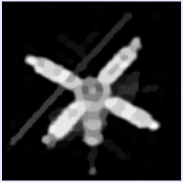

[FRAC. PSNR: 23.78dB ]

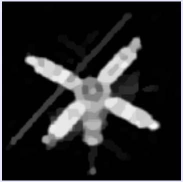

[TR-$\ell_p$. PSNR: 24.04dB]

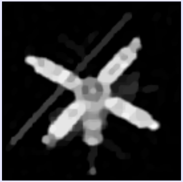

[TR-LN. PSNR: 24.04dB]

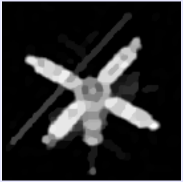

[TR-FRAC. PSNR:23.87dB]

# Numerical demonstration in 2D - experimental results

[Shepp-Logan. Size: $256 \times 256$]

[TV. PSNR: 26.66dB ]

[SCAD. PSNR: 27.67dB ]

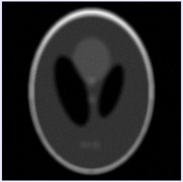

[Blurry & Noisy. PSNR: 19.02dB]

[TR-TV. PSNR: 27.38dB ]

[TR-$\ell_2$. PSNR: 24.86dB ]

# Numerical demonstration in 2D - experimental results

[ $\ell_p$. PSNR: 27.20dB]

[LN. PSNR: 27.55dB]

[FRAC. PSNR: 26.69dB ]

[TR-$\ell_p$. PSNR: 27.45dB]

[TR-LN. PSNR: 28.02dB]

[TR-FRAC. PSNR:27.30dB]

# Numerical demonstration in 2D
# - experimental results analysis

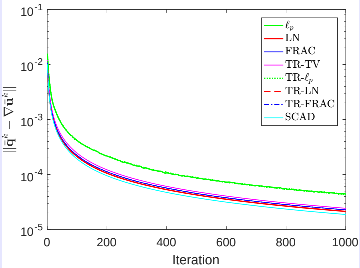


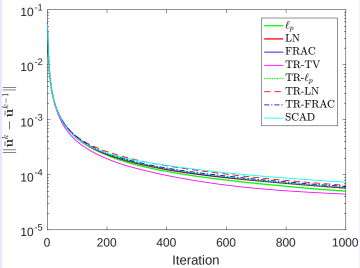


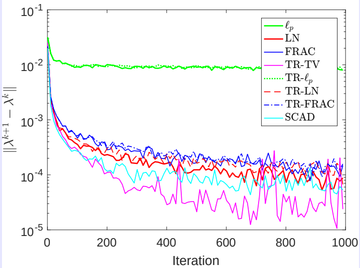

# Numerical demonstration in 2D - PSNR values

| TR-TV | | TR-$\ell_p$ | | TR-LN | | TR-FRAC | | SCAD | |
|---|---|---|---|---|---|---|---|---|---|
| $(\alpha,\beta) =$ (2000, 600) | | $(\alpha,\beta,p) =$ (5000, 5000, 0.5) | | $(\alpha,\beta,\theta) =$ (13000, 8000, 10) | | $(\alpha,\beta,\theta) =$ (8000, 6000, 10) | | $(\alpha,\beta) =$ (200, 100) | |
| $\tau$ | PSNR | $\tau$ | PSNR | $\tau$ | PSNR | $\tau$ | PSNR | $\theta(\tau = a\theta)$ | PSNR |
| 0.1 | 23.12 | 0.1 | 23.63 | 0.1 | 23.57 | 0.1 | 23.52 | 0.01 | 22.39 |
| 0.2 | 23.58 | 0.2 | 24.04 | 0.2 | 24.04 | 0.2 | 23.87 | 0.04 | 23.22 |
| 0.3 | 23.48 | 0.3 | 23.98 | 0.3 | 23.90 | 0.3 | 23.83 | 0.07 | 23.89 |
| 0.4 | 23.81 | 0.4 | 23.93 | 0.4 | 23.90 | 0.4 | 23.81 | 0.10 | 24.11 |
| 0.5 | 23.99 | 0.5 | 23.93 | 0.5 | 23.90 | 0.5 | 23.81 | 0.13 | 24.07 |
| 0.6 | 24.00 | 0.6 | 23.93 | 0.6 | 23.90 | 0.6 | 23.81 | 0.16 | 23.93 |
| 0.7 | 24.00 | 0.7 | 23.93 | 0.7 | 23.90 | 0.7 | 23.81 | 0.19 | 23.77 |
| 0.8 | 24.00 | 0.8 | 23.93 | 0.8 | 23.90 | 0.8 | 23.81 | 0.22 | 23.61 |
| 0.9 | 24.00 | 0.9 | 23.93 | 0.9 | 23.90 | 0.9 | 23.81 | 0.25 | 23.49 |
| 1.0 | 24.00 | 1.0 | 23.93 | 1.0 | 23.90 | 1.0 | 23.81 | 0.27 | 23.48 |

# Section 7. Conclusions

# Conclusions

- Any convex regularization, is impossible to recover the ground truth.
- Presented a general truncation regularization framework.
- Analysis in 1D theoretically to show better performance.
- Optimization in 2D with implementation and convergence.
- Experiments numerically showed advantages of our method.
- One future work is to design more efficient algorithms.

# Section 8. References

- Wu C. and Liu Z. and Wen S. A General Truncated Regularization Framework for Contrast-Preserving Variational Signal and Image Restoration: Motivation and Implementation. Accepted by Sci. China. Math. 2018.

- Guo K, Han D, and Yuan X. Convergence analysis of Douglas–Rachford splitting method for "strongly + weakly" convex programming. SIAM J Numer Anal, 2017, 55: 1549-1577.

- Wang Y, Yin W, and Zeng J. Global convergence of ADMM in nonconvex nonsmooth optimization. arXiv preprint arXiv:1511.06324v4, 2016.

- G Li and Pong T K. Global convergence of splitting methods for nonconvex composite optimization. SIAM J Optim, 2015, 25: 2434–2460.

- Hintermüller M and Wu T. Nonconvex TV$^q$-models in image restoration: Analysis and a trust-region regularization-based superlinearly convergent solver. SIAM J Imaging Sci, 2013, 6: 1385–1415.

- Xu Z, Chang X, Xu F, et al. $L_{1/2}$ regularization: A thresholding representation theory and a fast solver. IEEE Trans Neural Netw Learn Syst, 2012, 23: 1013–1027.

- Wu C and Tai X-C. Augmented lagrangian method, dual methods, and split Bregman iteration for ROF, vectorial TV, and high order models. SIAM J Imaging Sci, 2010, 3: 300–339.
- Nikolova M, Ng M K, and Tam C-P. Fast nonconvex nonsmooth minimization methods for image restoration and reconstruction. IEEE Trans Image Process, 2010, 19: 3073–3088.
- Wang Y, Yang J, Yin W, et al. A new alternating minimization algorithm for total variation image reconstruction. SIAM J Imaging Sci, 2008, 1: 248–272.
- Nikolova M. Analysis of the recovery of edges in images and signals by minimizing nonconvex regularized least-squares. Multiscale Model Simul, 2005, 4: 960–991.
- Rudin L I, Osher S, and Fatemi E. Nonlinear total variation based noise removal algorithms. Phys D, 1992, 60: 259–268.

# Thank you!